Radiation Resistant Quadrupole Magnet for the Super-FRS at FAIR

M. Winkler, M. Svedentsov, K.H. Behr, H. Geissel, H. Iwase, G. Moritz, C. Mühle, H. Weick

***Abstract*—The planned new international accelerator facility FAIR (Facility for Antiproton and Ion Research, [1]) at GSI will provide primary beams of all projectiles up to uranium with energies up to 1.5 GeV/u for nuclear structure physics. The maximum intensities of these projectile beams will be (1-3) □ 10^{12} /s, leading to a maximum beam power of 58 kW. 10-20% of the primary beam will react in a high-power production target at the entrance of the Super-FRS (Super-conducting Fragment Separator, [2]). The Super-FRS is a large-acceptance two-stage fragment separator which will provide spatially separated isotopic beams of exotic nuclei. The non-reacting primary beam will be dumped at dedicated beam catchers, located at well defined places in the first part of the Super-FRS.**

The target area as well as the beam dump area is in high fluxes of high-energy particles, mainly neutrons and protons. Since magnetic elements located in these areas have to be reliably operated for the lifetime of the facility (~20 years) their design has to be radiation resistant. Presently we consider building the magnet coils using MIC (Mineral Insulation Cable) technology. In this paper we present radiation issues, magnet specification, and possible magnetic designs of the first quadrupole magnet placed 1 m downstream of the production target.

***Index Terms*—High intensity accelerator, high intensity beams, fragment separator, mineral insulation cable, magnetic fields, radiation resistant magnet.**

I. Introduction

THE success of the present exotic nuclear beam facilities is the motivation for new projects and plans for next-generation devices worldwide. The new SIS 100/300 accelerator complex at FAIR will provide primary beam intensities of up to 10^{12} ions/s of ^{238}U at energies of 1500 MeV/u, which is a factor of 1000 more than presently available at GSI. The primary beam will impinge on a high power production target with a thickness of a few g/cm^2 where rare isotopes of all elements up to uranium will be produced. The fragment beams will be spatially separated within some hundred nanoseconds by the new two-stage fragment separator Super-FRS. The magnetic system of the Super-FRS will consist of three branches connecting different experimental areas as shown in Fig. 1. Since the Super-FRS has to accept fragment beams with a large phase-space volume all magnets must have large apertures.

In the production target approximately 10-20 % of the primary beam will react. The non-reacting primary beam will be stopped at localized beam dumps in the first separator stage (Pre-Separator), see also Fig. 1. At both positions the primary beam will be partially converted into heavier fragments and light particles, like protons and neutrons. Thus due to the high radiation level radiation resistant magnets have to be used in this part of the separator while anywhere else super conducting magnets will be applied.

One of the most crucial magnets concerning radiation resistance is the very first quadrupole PQ_{11} which is placed already 1 m behind the production target (see detail in Fig. 1). Its magnetic specifications are given in Table I.

TABLE I
SPECIFICATION OF THE QUADRUPOLE MAGNET PQ_{11}

Parameter	Units	Value
Effective length	m	1.0
Maximum field gradient	T/m	15.0
Minimum field gradient	T/m	1.5
Useable aperture	mm	±90
Pole tip radius	mm	100
Maximum pole tip field	T	1.5
Field gradient quality		$\pm 8 \cdot 10^{-4}$
Operation		DC-Mode

II. Radiation Issues

A. Energy deposition in the target area of the Super-FRS

Detailed Monte Carlo simulations using the PHITS code [3] were performed to estimate the radiation impact in the target area of the Super-FRS. Fig. 2 shows the results of these calculation, i.e. the energy deposition along the optic axis (left panel) and at the entrance surface (simplified) of quadrupole PQ_{11} (right panel), respectively. The calculation assumed a ^{238}U primary beam with an energy of 1500 MeV/u and an intensity of 10^{12} ions which is focused on a carbon target to a spot of σ_x = 1.0 mm and σ_y = 2.0 mm, respectively. The

Manuscript received September 20, 2005. The prototype development of this magnet is part of the European FP6 Design Study program under the contract number 515873 - 'DIRACsecondary-Beams'.

M. Winkler, K.-H. Behr, H. Geissel, H. Iwase, H. Weick are with GSI, department KP2, Planckstrasse 1, D-64291, Darmstadt, Germany. (emails: M.Winkler@gsi.de; K-H.Behr@gsi.de ;H.Geissel@gsi.de; H.Iwase@gsi.de; H.Weick@gsi.de, phone: 0049-6159-712468, fax: 0049-6159-712902)

G. Moritz, C. Muehle, are with GSI, department BTE, Planckstrasse 1, D-64291, Darmstadt, Germany. (emails: G.Moritz@gsi.de; C.Muehle@gsi.de, phone: 0049-6159-712368, fax: 0049-6159-712043).

M. Svedentsov is with the Inst. for Analytical Instrumentation, RAS, 198103, Rizhskijpr., 26, St.Petersburg, Russia (e-mail: msved@iai.rssi.ru).

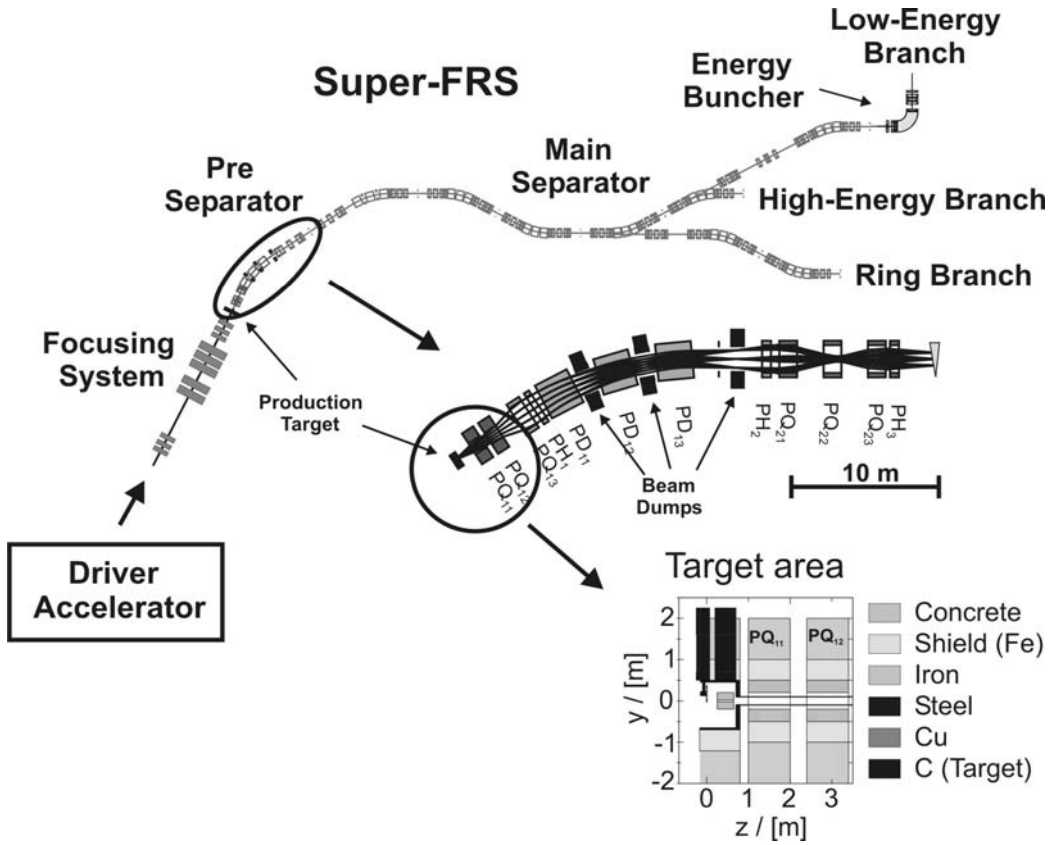

Fig. 1. Layout of the Super-FRS consisting of the Pre- and the Main-Separator. The magnetic elements after the production target and the beam dumps have to be radiation resistant. Details are shown for the target area.

momentum spread of the primary beam is $\sigma_P/P = 0.5$ %. The target has a thickness of d = 4 g/cm^2.

In average the energy deposition on the coil surface is $\langle\Delta E\rangle/M \approx 1$ mJ/g, which is equivalent to a dose rate of 1 Gy/s. Assuming a 4000 h/year operation time this sums up to an accumulated dose of 14 MGy/year.

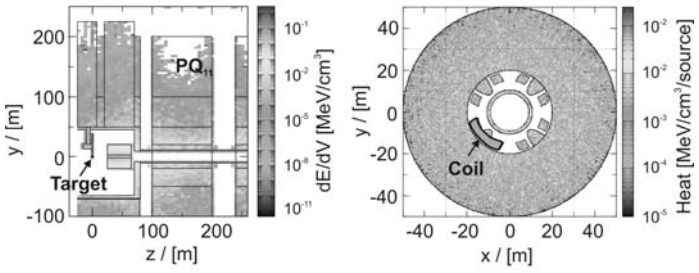

Fig. 2. Energy deposition per primary 1.5 GeV/u uranium ion impinging on a 4 g/cm^2 C target. The left side shows the distribution along the optic axis and the right side shows the distribution at the entrance surface of quadrupole PQ_{11}.

B. Choice of cable

Table II lists the radiation sensitivity of various conductor and insulator materials [4, 5]. The most crucial part is the coil insulation. To guarantee a long and save operation of the magnets over the whole lifetime of the facility (≈ 20 years) we consider in the moment to build them as normal conducting magnets using Mineral Insulation Cables (MIC). Such kinds of cables are nowadays available in various sizes, with or without hollow bores for different type of cooling scenarios (see Fig. 3).

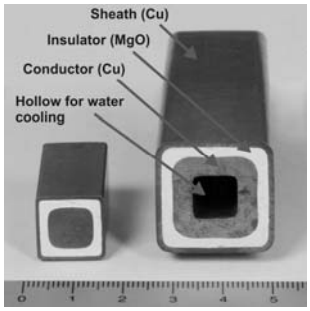

Fig. 3. Mineral Insulation Cable (MIC) as produced by HITACHI Cable Ltd.

TABLE II
RADIATION SENSITIVITY OF VARIOUS MATERIALS

Material	Radiation limit / [Gy]
NbTi	$\approx 5 \cdot 10^8$
Nb_3Sn	$\approx 5 \cdot 10^8$
Copper	$> 10^{10}$
Ceramics (Al_2O_3, MgO, etc)	$> 10^9$
Organics	10^6 -10^8

III. MAGNETIC DESIGN OF THE QUADRUPOLE PQ_{11}

A. 2D design: the quadrupole cross section

Two different magnetic designs of the quadrupole PQ_{11} were

performed. The first design uses the cable MIC 2500A-H assuming direct water cooling and the second uses MIC 1000A (or MIC 2000A) cable with indirect cooling. The advantage using the direct cooled cable is a higher possible current density and thus a more compact overall design. On the other hand the advantages of the indirect cooled coil are better mechanical properties of the cable and a slightly better field distribution in the aperture. Table III summarizes the parameters of the two designs.

TABLE III
QUADRUPOLE DESIGN PARAMETERS

Parameter	Design1	Design2
Cable type	MIC 2500A-H*	MIC 1000A*/ MIC 2000A*
Cable outer size	23.8 mm	18.0 mm / 14.0 mm
Conductor size	18.0 mm	16.6 mm / 12.6 m
Number of turns	26	92 / 46
Correcting turns	3	2 / 1
Maximum current	72.5 kA	94.4 kA
Engineering current density	4.34 A/mm^2	2.5 A/mm^2
Iron weight	11.8 ton	14.9 ton
Coil weight	1.1 ton	depends on cooling design

*Product name of HITACHI Cable Ltd.

The cross section of the iron yoke and the position of the coil were optimized to provide the required field quality inside the good field area. The negative effect of the yoke saturation may be partly compensated by introducing air slots in the pole [6], which should be easy to implement from mechanical point of view, since we intend to use laminated iron. These slots imitate the saturation of the pole's central part at high flux density levels and homogenize the field distribution in the aperture.

In both magnet designs the coil consists of two parts, the main coil and a pole-tip (correcting) block of few turns. Fig. 4 shows the optimized cross section (1/8 part) of the two designs, including details of the pole shape with correction coils. The lower part of Fig. 4 demonstrates that for all excitation currents the maximum field gradient deviation satisfies the requirements and stays within the margins of $\pm 8\times10^{-4}$ relative units.

All the presented results have been obtained using the program OPERA-2D.

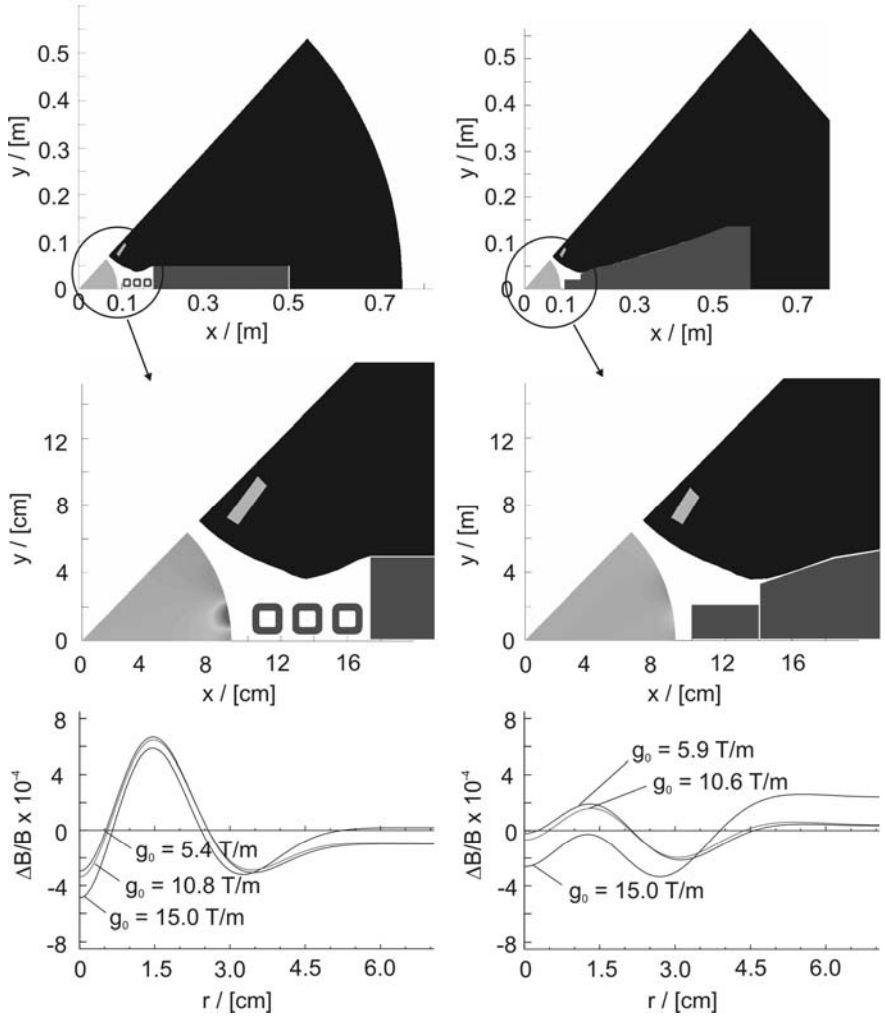

Fig. 4. Cross section (1/8 part) of the two investigated quadrupole designs and the resulting field homogeneity. The left panel shows the design using the MIC 2500A-H cable (direct water cooling) while the right panel shows the design using the MIC1000A or MIC 2000A cable (both cables are indirectly cooled).

B. 3D investigations

The described quadrupole designs provide the desired field quality only in the middle part of the magnet. The integral focusing effect of the magnet depends also on the field distribution near the end parts of the magnet. For this reason we investigated also the 3D properties of the first quadrupole design using the direct cooled cable (MIC 2500A-H). The magnet yoke in the 3D model was built by simply extruding the 2-D cross section model (see Fig. 5). The coil ends were simulated to be saddle shape; both the main coil as well as the corrector coil (see Fig. 6).

The 3D simulation of the magnetic field indicates that the integral field quality of this quadrupole is only slightly worse compared to the 2D calculation and still stays within the limits of the requirements. Fig. 7 demonstrates the field quality in the midplane of the quadrupole magnet at the maximum field gradient (g = 14.7 T/m). The different curves belong to the field distribution at different radii (from 50 to 80 mm). It should be noted that especially the shape of the distribution is changed compared to the 2D calculations.

Fig. 5. 3D design of the quadrupole PQ_{11} using the direct cooled cable MIC 2500A-H.

Fig. 6. 3D model of the coil. Main coil as well as corrector coil are saddle-shaped.

All 3-dimensional calculations of the static magnetic field were performed using the software OPERA-3D (TOSCA).

IV. Conclusions

Two magnetic designs for the first quadrupole magnet placed 1 m behind the production target of the Super-FRS are presented. All designs use MIC cable in order to increase radiation resistance. All presented versions achieve the required field homogeneity of $\pm 8 \cdot 10^{-4}$ in the quadrupole aperture of ±90 mm for field gradients varying from 1.5 T/m up to 15 T/m. The field quality for high field gradients is achieved with the help of air slots in the yoke, capable of partly compensating saturation effects. 3D simulations indicate a change of the distribution of the field homogeneity compared to 2D calculations; however, the results still stay within the requirements.

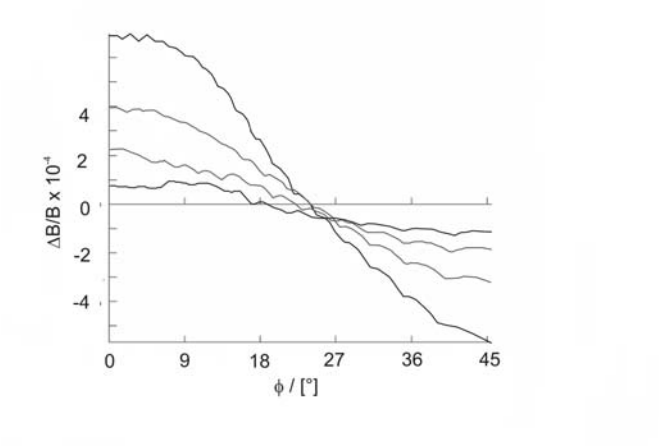

Fig. 7. Field quality in the midplane of the quadrupole for a field gradient of g = 14.7 T/m. The curves belong to the distribution along the radii 50 mm (smallest deviation), 60 mm, 70 mm, and 80mm (largest deviation), respectively.

References

[1] An International Accelerator Facility for Beams of Ions and Antiprotons, Conceptual Design Report, GSI (2001), http://www.gsi.de/GSI-Future/cdr/

[2] H. Geissel et al, Nucl. Instr. and Methods B 204 (2003) 71.

[3] H. Iwase, K. Niita, and Takashi Nakamura, Journal of Nuclear Science and Technology, Vol. 39, No. 11, pp. 1142-1151, (2002).

[4] M. Sawan et al, Fusion Technology 10 (1986) 741.

[5] R. Reed and D. Evans, "Insulation systems for the Muon Colliders", unpublished report (2000).

[6] A. Chernosvitov, A. Kalimov, H. Wollnik, IEEE Trans. Appl. Supercond., vol. 12, pp. 1430-1433, March 2002.